Available online at www.sciencedirect.com

ScienceDirect

journal homepage: www.elsevier.com/locate/he

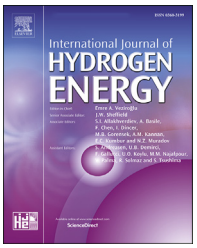

Pathways to low-cost clean hydrogen production with gas switching reforming

Shareq Mohd Nazir [a,b,*], *Jan Hendrik Cloete* [c], *Schalk Cloete* [c], *Shahriar Amini* [a,c,**]

[a] *Department of Energy and Process Engineering, Norwegian University of Science and Technology, Trondheim, Norway*

[b] *KTH Royal Institute of Technology, Stockholm, Sweden*

[c] *SINTEF Industry, Trondheim, Norway*

HIGHLIGHTS

- Hydrogen plant with gas switching reforming is optimised for efficiency and cost.
- GSR-H2 can achieve negative specific primary energy consumption for CO_2 avoided.
- GSR-H2 produces 4.5% cheaper H_2 with 96% CO_2 capture at 15 $ per ton CO_2 avoided.
- GSR-H2 technology is robust to almost any future energy market scenario.
- Oxygen carrier stability is critical for techno-economic performance of GSR-H2 plant.

ARTICLE INFO

Article history:
Received 29 November 2019
Received in revised form
18 January 2020
Accepted 26 January 2020
Available online xxx

Keywords:
Hydrogen production
CO_2 capture
Natural gas reforming
Techno-economic assessment
Gas switching reforming

ABSTRACT

Gas switching reforming (GSR) is a promising technology for natural gas reforming with inherent CO_2 capture. Like conventional steam methane reforming (SMR), GSR can be integrated with water-gas shift and pressure swing adsorption units for pure hydrogen production. The resulting GSR-H2 process concept was techno-economically assessed in this study. Results showed that GSR-H2 can achieve 96% CO_2 capture at a CO_2 avoidance cost of 15 $/ton (including CO_2 transport and storage). Most components of the GSR-H2 process are proven technologies, but long-term oxygen carrier stability presents an important technical uncertainty that can adversely affect competitiveness when the material lifetime drops below one year. Relative to the SMR benchmark, GSR-H2 replaces some fuel consumption with electricity consumption, making it more suitable to regions with higher natural gas prices and lower electricity prices. Some minor alterations to the process configuration can adjust the balance between fuel and electricity consumption to match local market conditions. The most attractive commercialization pathway for the GSR-H2 technology is initial construction without CO_2 capture, followed by simple retrofitting for CO_2 capture when CO_2 taxes rise, and CO_2 transport and storage infrastructure becomes available. These features make the GSR-H2 technology robust to almost any future energy market scenario.

* *Corresponding author*. KTH Royal Institute of Technology, Teknikringen 42, Stockholm 11428, Sweden.
** *Corresponding author*. Kolbjørn Hejes vei 1b, Dept. of Energy and Process Engineering, NTNU, NO-7491 Trondheim, Norway.
E-mail addresses: shareq.m.nazir@ntnu.no, smnazir@kth.se (S.M. Nazir), shahriar.amini@ntnu.no (S. Amini).

https://doi.org/10.1016/j.ijhydene.2020.01.234

Nomenclature

ASU	Air Separation Unit
ATR	Auto-Thermal Reforming
BEC	Bare Erected Cost
CA	CO_2 Avoided
CC	CO_2 Captured
CCS	Carbon Capture and Storage
CCUS	Carbon Capture Utilization and/or Storage
CEPCI	Chemical Engineering Plant Cost Index
CF	Capacity Factor
CHP	Combined Heat and Power
CLC	Chemical Looping Combustion
CLR	Chemical Looping Reforming
COCA	Cost of CO_2 Avoidance
CSTR	Continuous Stirred Tank Reactor
EPCC	Engineering Procurement and Construction Cost
FC	Fuel Cost
FCF	Fixed Charge Factor
FOM	Fixed Operating and Maintenance
FTR	Fired Tubular Reformer
GSR	Gas Switching Reforming
GSR-CC	Gas Switching Reforming Combined Cycle
GSR-H2	Gas Switching Reforming Hydrogen plant
IEA	International Energy Agency
IPCC	Inter-governmental Panel on Climate Change
LHV	Lower Heating Value
NG	Natural Gas
NGCC	Natural Gas Combined Cycle
PSA	Pressure Swing Adsorption
SMR	Steam Methane Reforming
SPECCA	Specific Primary Energy Consumption for CO_2 Avoided
S/C	Steam to Carbon mole ratio
TIT	Turbine Inlet Temperature
WGS	Water-Gas Shift

Symbols

η_{H_2}	Hydrogen Production Efficiency
η_{eq,H_2}	Equivalent Hydrogen Production Efficiency
E_{CO2}	CO_2 emission intensity from the process
E_{el}	Avoided CO_2 intensity of electricity export/import
E_{eq,CO_2}	Equivalent CO_2 emission intensity from the process
E_{NG}	CO_2 emission intensity of NG combustion
E_{th}	Avoided CO_2 intensity of thermal energy exports (steam export)
$\dot{m}_{eq,NG}$	Equivalent mass flow rate of NG
$\dot{m}_{H2}$	Mass flow of hydrogen produced
$\dot{m}_{NG}$	Mass flow of NG
$\dot{m}_{CO2}$	Mass flow of CO_2 emitted
P_1	Pressure of PSA inlet stream
P_2	Pressure of PSA off-gas stream from PSA
Q_{th}	Thermal energy export in the form of 6 bar steam
r	Interest or discount rate
W_{el}	Net electrical power

Introduction

Anthropogenic CO_2 emissions have been the dominant cause of observed global warming from the middle of 20th century [1]. The International Energy Agency (IEA) presented different pathways and their contributions to mitigate these emissions, of which, fuel switching and carbon capture and storage (CCS) accounts for reduction of 5% and 14% (respectively) of the cumulative global CO_2 emissions by 2060 in the defined 2° scenario [2]. When global temperatures must be restricted below 1.5 °C [3], the Intergovernmental Panel on Climate Change (IPCC) presented scenarios with more emphasis on hydrogen and carbon capture utilization and/or storage (CCUS) as pathways to mitigate CO_2 emissions.

Hydrogen is attracting increasing attention as a carbon-free energy carrier in industry, transport and power sector, exemplified by a recent IEA special report [4]. In this report, natural gas reforming with conventional CCS remains economically more attractive than electrolytic hydrogen production in most regions over coming decades. This assessment does not account for a next generation of natural gas reforming technologies with integrated CO_2 capture that have the potential to achieve similar costs to reference plants without CO_2 capture (e.g. membrane-assisted reforming technologies [5]). Another such technology is assessed in this study: gas switching reforming (GSR).

The demand for hydrogen has been on a rise since 1975 as seen in Fig. 1, mainly in the ammonia and oil refining sector. It is predicted to further increase with favorable policy directives for hydrogen deployment, especially in the transport sector [4]. 76% of the current hydrogen in the world is produced from natural gas (NG) reforming that results in 10 ton of CO_2 emitted per ton of H_2 produced [4]. The IEA predicts that NG will overtake coal in 2030 to become the second largest fuel (after oil) in global energy mix, of which the industrial consumers will contribute to a 45% increase in worldwide gas use [6]. In this scenario, hydrogen production from NG with CCUS, which is the focus of this study, provides an attractive clean energy alternative. Hydrogen also provides an opportunity to use existing gas infrastructure for new clean hydrogen supplies [4], especially related to transport and storage of it.

A detailed review on different hydrogen production methods integrated with CO_2 capture was presented by Voldsund et al. [7]. In conventional hydrogen production process, NG is first converted to syngas via steam methane reforming (SMR) in fired tubular reformer (FTR) or auto-thermal reformer (ATR). FTR uses external firing to provide heat for the reaction whereas in ATR, a fraction of the fuel is combusted internally to provide heat. Syngas is converted to CO_2 and H_2 in subsequent water-gas shift (WGS) reactors. Pure hydrogen is recovered in a pressure swing adsorption (PSA) step and the off-gas is combusted either to provide heat for reforming reaction or in a combined heat and power (CHP) unit. SMR with FTR is currently the dominant technology to produce large scale pure hydrogen from NG due to its favorable economics [4]. In the SMR process, CO_2 can be captured from the upstream or downstream of H_2 recovery step (reducing CO_2 emissions by 60%) or the exhaust gases from FTR burners (reducing CO_2 emissions by 90%). Each of these

Please cite this article as: Nazir SM et al., Pathways to low-cost clean hydrogen production with gas switching reforming, International Journal of Hydrogen Energy, https://doi.org/10.1016/j.ijhydene.2020.01.234

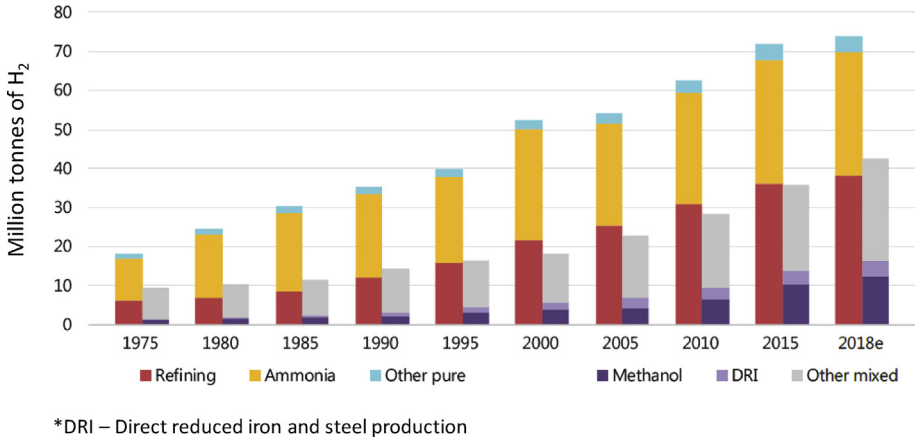

Fig. 1 – Trends in global demand for hydrogen [4].

gas streams has different conditions with respect to partial pressure of CO_2 and the total mass flow of CO_2. Soltani et al. [8] reported that capturing CO_2 at the upstream of the H_2 recovery step is more favorable for the design conditions (Steam/Carbon mole ratio of 2.5–3 and reformer temperature of 890 °C) in the conventional SMR plant. However, when CO_2 is captured from the exhaust gases of FTR to obtain ~80% CO_2 avoidance, the equivalent hydrogen production efficiency of the SMR process drops by 14 %-points when compared to the reference plant and thereby increasing the cost of hydrogen by 30% [5]. The penalty is due to capturing CO_2 from dilute flue gases that contain mostly N_2. Similar penalty is also reported for methane-cracking technology studied by Abanades et al. [9] to produce clean hydrogen, but in this process the main challenge is with handling of carbon deposits. This penalty is minimized in ATR based H_2 production process by having an air separation unit (ASU) that feeds in pure oxygen for reforming and boiler sections [10]. The flue gas stream contains only CO_2 and H_2O, from which, H_2O is condensed leaving pure CO_2 stream for transport and storage. Although the penalty in capturing CO_2 is only ~2%-points in the ATR based process, it requires an additional ASU that has high capital costs alongside leaving the N_2 stream that is not used in the process. Therefore, ATR is more suited for ammonia production that does need separation of N_2 in ASU [11]. The hydrogen production costs from these two technologies are sensitive to the NG price and the CO_2 tax (when comparing with options with CO_2 capture) [12].

Membrane and sorption enhanced reactors are alternatives for integrated syngas production and gas separation [7]. These methods can be applied to either SMR or WGS steps. WGS and SMR membrane reactors separate the H_2 whereas sorption enhanced WGS or SMR reactors separate CO_2. The membrane reactors produce pure H_2 leaving an impure CO_2 stream, and the sorption enhanced reactors produce high quality CO_2 stream for transport and storage but a low purity H_2 stream. In addition, membranes are cost intensive and the sorption enhanced system requires highly active solid sorbents for higher hydrogen production efficiencies [13]. Pressurized sorption enhanced systems may have lower costs due to compact systems and lower work required for H_2 and CO_2 compression, but the equivalent hydrogen efficiency is lower. A variant of sorption enhanced hydrogen production system is the Ca-Cu looping process that consists of three stages, the sorption enhanced reforming, Cu oxidation with air and CuO reduction alongside $CaCO_3$ calcination. The Ca-Cu looping process for hydrogen production exhibits specific primary energy consumption for CO_2 avoided (SPECCA) of 1.07–1.54 MJ/kg-CO_2 depending on the pressure inside the reactor [14]. It can capture ~96% CO_2 at 31 €/ton cost of CO_2 avoided. However, the cost of hydrogen produced using Ca-Cu looping process is 16% higher than in SMR plant without capture [14].

Chemical looping reforming (CLR) systems show higher potential to produce syngas and inherently separate air [15]. A schematic of a typical CLR system is shown in Fig. 2a. NG and steam are reformed in the fuel reactor of the CLR to produce syngas in the presence of an oxidised metallic oxygen carrier. The oxygen carrier is reduced and sent to the oxidation reactor where it is oxidised by the air stream, leaving a depleted air stream that mainly contains N_2. In addition, Kang et al. [16] analysed a three-reactor chemical looping reforming system comprising of air, fuel and steam reactors. The oxidised metal oxide (oxygen carrier) from the air reactor is partially reduced in the fuel reactor with methane forming CO_2 and H_2O, and the remaining reduction of the metal oxide happens in the steam reactor where steam reduces the oxygen carrier to form H_2. One of the main practical challenges with these CLR systems is their scale-up for pressurized interconnected operation, which is needed for higher process efficiency [17]. When CLR is integrated in a process for gas-fired power production, it needs to be operated between 18 and 20 bar [18], whereas hydrogen production processes require even higher pressures [17].

To address the challenge with respect to circulation of oxygen carrier between inter-connected reactors in chemical looping, several other reactor configurations including packed bed chemical looping [19,20], rotating bed reactor [21] and gas switching reactor [22,23] have been developed and presented in literature for combustion or reforming of fuel. The present study focuses on the application of gas switching to NG reforming to produce hydrogen. A schematic of the gas switching reforming (GSR) system is shown in Fig. 2b. The oxygen carrier (Ni-NiO system in this study) is kept inside the

Please cite this article as: Nazir SM et al., Pathways to low-cost clean hydrogen production with gas switching reforming, International Journal of Hydrogen Energy, https://doi.org/10.1016/j.ijhydene.2020.01.234

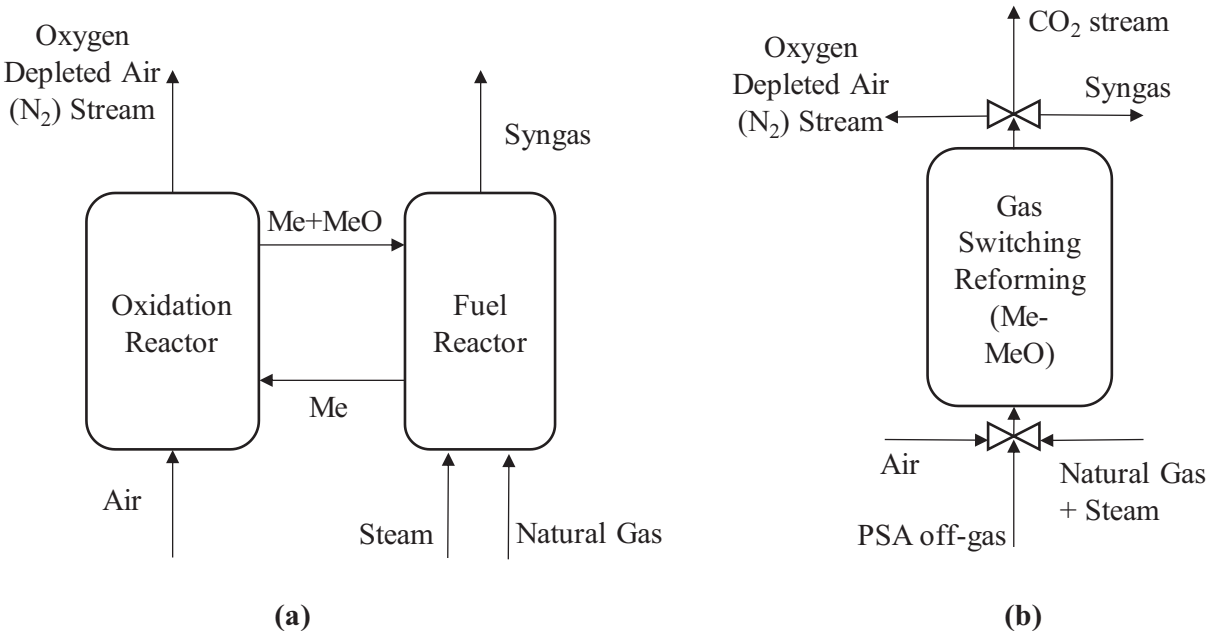

Fig. 2 – Schematic of a) Chemical looping reforming b) Gas switching reforming.

bubbling fluidized bed reactor, and the gas streams alternate during different oxidation, reduction and reforming stages. The air stream oxidises the oxygen carrier, producing an oxygen depleted air stream (N_2 stream) during the oxidation step. Subsequently, the oxygen carrier is reduced by the off gases from the pressure swing adsorption (PSA) unit during the reduction step. The reduced oxygen carrier then acts as a catalyst for the steam-methane reforming in the third step of the GSR process. There is no circulation of oxygen carrier between reactors that eliminates the challenges with loop seals and cyclones. GSR also allows for easy integration of the PSA unit to recover high purity hydrogen and use the off-gases in the reduction step. However, GSR requires high temperature inlet and outlet valves to switch gases between different stages. In addition, GSR needs a cluster of reactors to provide steady product output from the process [24].

The GSR reactor was experimentally demonstrated by Wassie et al. [23], where the effect of reactor temperature and cycle times (for oxidation, reduction and reforming steps) on the conversion of methane was reported. A 1D phenomenological model for GSR was developed to understand the flow, temperature and conversion profiles inside the reactor [25] and compared against the conventional CLR process. GSR has lower fuel conversion but produces syngas with higher heating value. Following this, the potential of GSR process integrated with combined cycle gas-fired power production and CO_2 capture, a process defined as Gas Switching Reforming Combined Cycle (GSR-CC), was presented by Nazir et al. [24,26]. GSR-CC has an efficiency penalty of only 7.2%-points with respect to the reference Natural Gas Combined Cycle (NGCC) power plant alongside avoiding more than 95% of CO_2 [24]. Since GSR-CC produces a steady stream of 99.999% pure H_2 for combustion in a gas turbine to generate electricity, it gives an opportunity to stop the power cycle and export pure hydrogen in times of excess variable renewable electricity. When capitalizing on this flexibility, GSR-CC offers higher economic returns while operating at the low capacity factors required to balance variable renewables when compared to NGCC plants with post combustion CO_2 capture [27].

Although GSR-CC looks like a promising concept to produce power, GSR process is more likely to get deployed for pure hydrogen generation considering the scales of the plant. GSR was integrated with CO_2 capture for pure hydrogen production in a process designated as GSR-H2 [17], and its technical performance was compared against the conventional SMR process. In case of no CO_2 capture, GSR-H2 has nearly 3%-points higher equivalent hydrogen production efficiency when compared to SMR. In addition, GSR-H2 with more than 96% CO_2 capture faces an efficiency penalty of only 0.3%-points when compared to SMR plant without capture. However, GSR-H2 process consumes more electricity and hence, the source of electricity is critical for the performance of the GSR-H2 process. This will not only affect the efficiency of the process but will also affect the cost of hydrogen. In future energy scenarios, the cost of NG and CO_2 tax are expected to increase that will also have an impact on the cost of hydrogen produced [28]. A first of its kind techno-economic analysis revealed that GSR-H2 has the potential to produce hydrogen with similar costs to that from SMR plant without capture [29]. However, there is still a gap in literature with respect to the detailed techno-economic performance of the GSR-H2 process and its performance in future energy scenarios (for example: availability of cheap renewable electricity, CO_2 tax uncertainty etc). This paper improves upon the previous work on GSR-H2 process [17,29] and fills the gap in literature by carrying out process efficiency improvement studies of the GSR-H2 process through design changes, detailed techno-economic analysis and presenting scenarios for deployment of this technology. Equivalent hydrogen production efficiency, CO_2 avoidance, cost of CO_2 avoidance and levelised cost of hydrogen are the

Please cite this article as: Nazir SM et al., Pathways to low-cost clean hydrogen production with gas switching reforming, International Journal of Hydrogen Energy, https://doi.org/10.1016/j.ijhydene.2020.01.234

key performance indicators for techno-economic assessment of the GSR-H2 technology. The results have been compared against the reference SMR plant.

Process description of reference plant, base case GSR-H2 and improved GSR-H2 process

Reference steam methane reforming (SMR) plant

The conventional SMR plant for hydrogen production has been described previously in literature [5,13]. NG is desulphurized, mixed with steam and pre-heated for pre-reforming step to convert higher hydrocarbons into CH_4. The steam and CH_4 mixture (steam to carbon ratio of 2.70) is sent for reforming inside a catalytic fired tubular reformer (FTR), where more than 80% of CH_4 is converted to form syngas. CO and H_2O in the syngas are converted to CO_2 and H_2 in the WGS reactor before H_2 is separated in the PSA. Pure H_2 recovered from the PSA is compressed for transport and storage, whereas the PSA off-gas is combusted in the FTR burners to provide necessary heat for the reforming step. There is a lot of heat available in the process which is recovered to produce superheated high-pressure steam. A fraction of the steam is used in reforming and the remainder is expanded in steam turbines to generate electricity. The SMR plant simulation has been reproduced in this study, using the modelling assumptions in Nazir et al. [17], to maintain consistency in results obtained.

Base case GSR-H2 process

The schematic of the base case GSR-H2 is shown in Fig. 3. The pre-reforming section is similar to the SMR plant with a slightly lower steam to carbon (S/C) ratio of 2.66 at the inlet of the reforming step of the GSR. The outlet from the pre-reformer is pre-heated to 825 °C and fed to the GSR. GSR is designed at 32.7 bar, similar to the pressure conditions in the FTR in SMR plant. Syngas from the reforming step of GSR is cooled to 302 °C and sent to WGS step to convert nearly 77%-mol of CO into CO_2 and H_2O into H_2. The syngas from the WGS reactor is cooled to 25 °C to condense all the water from the stream to avoid degradation of the PSA adsorbents. 87.9% of H_2 is recovered in the PSA and compressed in three stages until 150 bar and 25 °C for transport and storage [5]. The off-gas from the PSA is compressed and pre-heated to 1000 °C before being fed to the GSR for the reduction step. The reduction step product gas contains only CO_2 and H_2O. H_2O is condensed and the CO_2 stream is compressed until 110 bar and 25 °C for transport and storage. Compressed air oxidises the oxygen carrier during the oxidation step of the GSR leaving the depleted air stream containing mainly N_2. The N_2 stream from the GSR is cooled and expanded in a gas turbine to generate electricity. There is a lot of heat that can be recovered from the process to pre-heat the process streams as well as prepare steam for reforming. The heat recovered in cooling the syngas from the GSR is used to pre-heat the NG and steam mixture at the inlet of the GSR, pre-reformer inlet and NG before the desulphurization step. The WGS product and the N_2 stream from the oxidation step of GSR are cooled down to generate steam for reforming. The outlet from the reduction step of the GSR that mainly contains CO_2 and H_2O, preheats the PSA off-gas that is fed to the GSR. The remaining heat in the reduction stage outlet is also used to generate steam for reforming.

The GSR-H2 process has higher electrical consumption when compared to the SMR plant. This is due to the work required for compressing air and CO_2 streams in addition to the H_2 stream as in SMR plant. Therefore, the source of electricity affects the overall process performance of GSR-H2. Efficient electricity source like NGCC results in higher equivalent hydrogen production efficiency of GSR-H2, whereas using a standalone NG boiler to fulfil electricity demand might result in an additional 2%-point efficiency penalty [17]. In addition to the efficiency penalty, the CO_2 avoidance also reduces. The sensitivity of levelised cost of hydrogen from GSR-H2 with respect to the source and cost of electricity is discussed later in this paper.

Improvements in design of GSR-H2 process

Four different designs of the GSR-H2 process are proposed to improve its techno-economic performance. In case 1, steel rods are inserted inside the GSR to increase the overall heat capacity of the GSR reactor system. This added thermal mass minimizes the temperature drop during the endothermic reforming step, achieving a higher average reforming temperature to lower the S/C ratio required for high fuel conversion. In case 2, a two-phase evaporator [24] is considered to produce steam for reforming using the steam condensation enthalpy in the CO_2 stream from the GSR reduction step that would otherwise be rejected. Case 3 is a combination of the above two designs, and case 4 presents an alternative heat integration strategy for the N_2 stream from the GSR oxidation step to increase H_2 production at the cost of increased power consumption. These designs are discussed briefly below.

Case 1: GSR with additional thermal mass
The GSR reactor is assumed to be inserted with steel rods to double the heat capacity in the reactor, which requires about 25% of the reactor volume to be occupied with steel rods [17]. This modification results in overall higher temperatures in different stages of GSR. Therefore, required conversion of methane is achieved at lower S/C ratios [17]. The main difference between the base case GSR-H2 process (as shown in Fig. 3) and this case is that the steam required for reforming is generated completely from cooling the WGS product (Boiler 1 in Fig. 3) and the GSR reduction stage outlet streams (Boiler 2 in Fig. 3). Therefore, the N_2 stream from the GSR oxidation stage is directly expanded in the turbine to generate a larger quantity of electricity. The remaining heat in the N_2 stream after expansion is recovered to generate saturated 6 bar steam for export.

Case 2: GSR-H2 process with two-phase evaporator to generate steam
In this case, the GSR reactor system is similar to the base case, without any additional thermal mass. A two-phase evaporator is used to generate steam for reforming while recovering heat from the GSR reduction stage outlet. The base case GSR-H2

Please cite this article as: Nazir SM et al., Pathways to low-cost clean hydrogen production with gas switching reforming, International Journal of Hydrogen Energy, https://doi.org/10.1016/j.ijhydene.2020.01.234

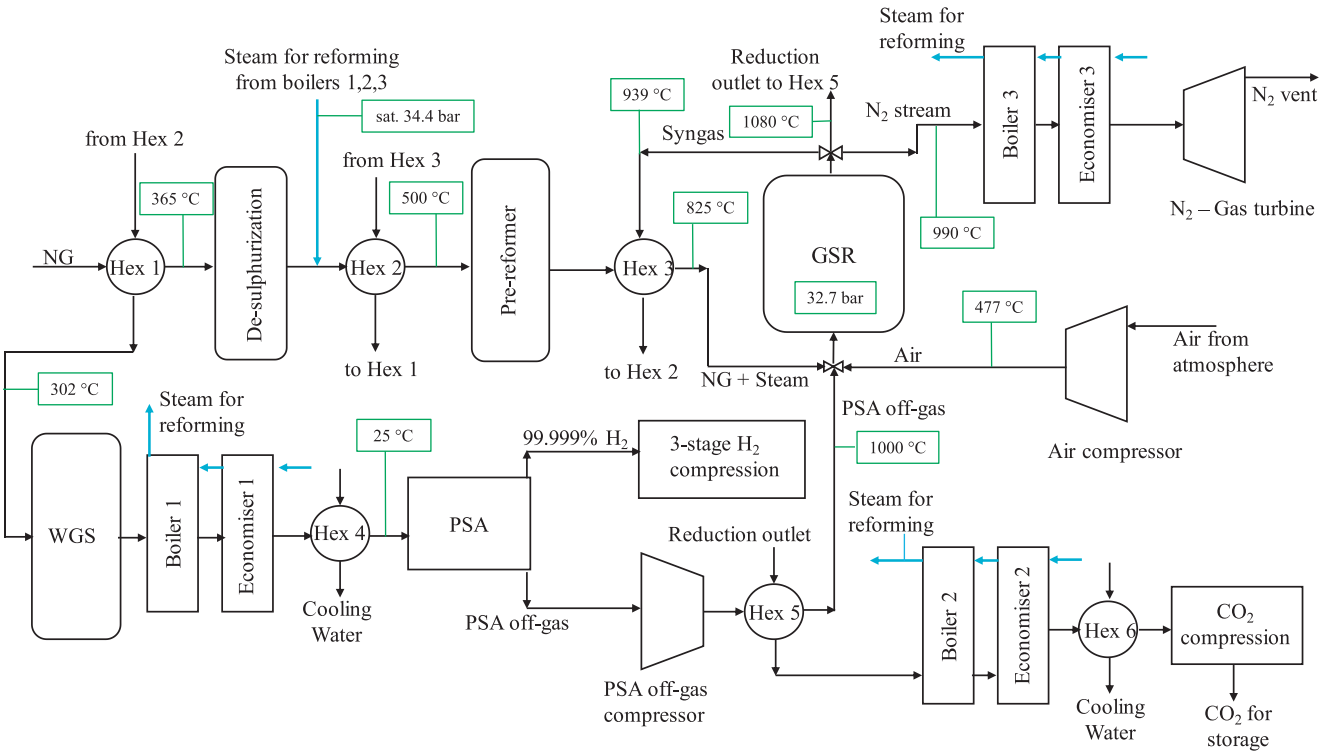

Fig. 3 – Schematic of base case GSR-H2 process (reproduced from Ref. [17]).

process needs to be modified to include this design change. NG is pre-heated for desulphurization with the desulphurized NG stream and the N_2 stream from the GSR oxidation step. The desulphurized NG and pressurized water stream is sent to the two-phase evaporator with the GSR reduction step outlet stream on the hot side of the evaporator. The water evaporates at low temperatures due to the presence of non-condensable fuel gases that reduce the steam partial pressure in the stream, allowing the steam condensation enthalpy in the CO_2 stream to be efficiently used for steam generation. The NG-steam mixture is then mixed with additional remaining steam, which is generated by recovering heat from the WGS product and N_2 stream, before being sent for pre-heating followed by pre-reforming step. Considering these modifications, the GSR-H2 process in case 2 would not have Economiser 2 and 3 and Boiler 2 as shown in Fig. 3, but instead have a two-phase evaporator. The Hex 1 in Fig. 3 is also replaced with two heat exchangers, where NG exchanges heat with desluphurized NG and N_2 stream.

Case 3: GSR-H2 process with additional thermal mass and two-phase evaporator

The GSR-H2 in case 3 is a combination of cases 1 and 2. Desulphurized NG and water mixture is passed through the two-phase evaporator that recovers steam condensation enthalpy from the GSR reduction step outlet. The GSR reduction step also operates at a higher average temperature, allowing for a lower S/C ratio (lower heat requirement for steam generation). The hot N_2 stream from the oxidation step of GSR is expanded in the gas turbine to generate electricity. Remaining heat in the N_2 stream after expansion is recovered to generate saturated 6 bar steam for export.

Case 4: GSR-H2 process as in case 3 in addition to pre-heated air for oxidation step of GSR

Case 3 is modified by including an air pre-heating step before the GSR oxidation stage so that the heat available in the process is directed towards higher conversion of methane in the GSR instead of high power production from expanding the N_2 stream at a high temperature. This configuration also eliminates the need to export a substantial amount of heat as low-value 6-bar steam. The design in case 4 is defined as advanced GSR-H2 process. The schematic of the advanced GSR-H2 process is shown in Fig. 4.

Methodology and assumptions

This section is presented in three parts. The first two parts describe the modelling methodology and assumptions in developing the 0D model for the GSR and the process model for the reference SMR plant and GSR-H2 process. The third part describes the methodology and assumptions used to carry out the techno-economic assessment of the GSR-H2 process.

0D model for the GSR

The transient gas switching reforming process is simulated using a 0D model coded in Matlab R2018b. The model solves the mass and energy balances of the system, assuming continuous stirred tank reactor (CSTR) behaviour of the reactor and that chemical- and thermal equilibrium are reached. These assumptions are reasonable considering the excellent mixing behaviour of fluidized bed reactors, the fast

Please cite this article as: Nazir SM et al., Pathways to low-cost clean hydrogen production with gas switching reforming, International Journal of Hydrogen Energy, https://doi.org/10.1016/j.ijhydene.2020.01.234

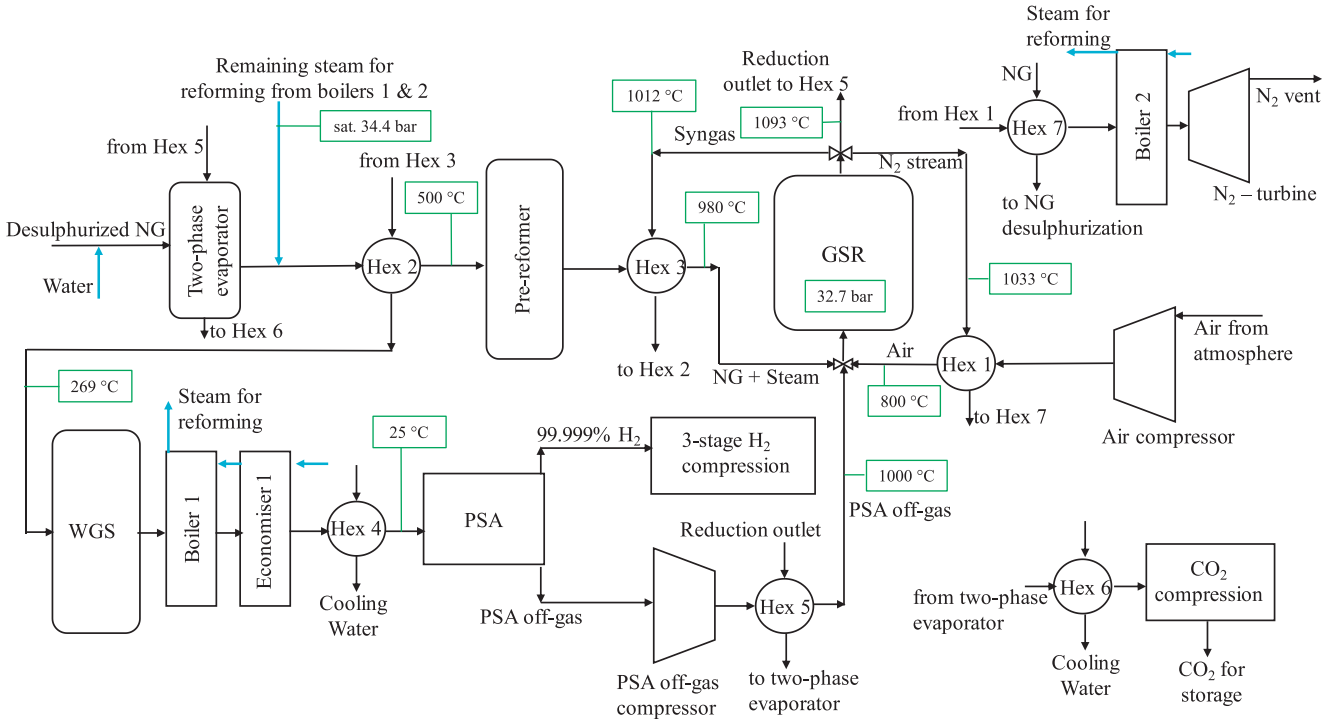

Fig. 4 – Schematic of advanced GSR-H2 process as described in Case 4.

reaction kinetics of the NiO oxygen carrier that is considered and the large geometries of industrial-scale fluidized beds [17]. This reactor model has been used in several previous studies [17,24,26], therefore the detailed model description is not repeated here. The interested reader is referred to these earlier studies for a complete description of the equations that are solved and the coupling between the reactor and process models.

The reactions occurring inside the GSR reactor are listed below. Eqs. (1)–(3) occur during the reduction step, Eq. (4) in the oxidation step, and Eqs. (5)–(7) in the reforming step.

$$CH_4 + 4NiO \rightarrow 4Ni + CO_2 + 2H_2O \quad (1)$$

$$H_2 + NiO \rightarrow Ni + H_2O \quad (2)$$

$$CO + NiO \rightarrow Ni + CO_2 \quad (3)$$

$$O_2 + 2Ni \rightarrow 2NiO \quad (4)$$

$$CH_4 + H_2O \leftrightarrow CO + 3H_2 \quad (5)$$

$$CO + H_2O \leftrightarrow CO_2 + H_2 \quad (6)$$

$$CH_4 + 2H_2O \leftrightarrow CO_2 + 4H_2 \quad (7)$$

The GSR reactors are operated similar to a previous study [17]. Firstly, the air flow rate is controlled to maintain a maximum reactor temperature of 1100 °C to prevent degradation of the oxygen carrier. The percentage oxygen carrier utilization is set equal to the reactor pressure in bars, which is kept constant at 32.7 bar for all cases considered here. The switching of the outlet valves between steps is slightly delayed compared to the switching of the inlet valves, since it has been shown that such a strategy reduces the undesired mixing between different reactor steps [30]. The ratio of the stage times of the reduction, reforming and oxidation steps (and therefore also the ratio of the number of reactors operating in each step) is specified as 1:3:1. This ratio results in similar outlet flow rates during each of the steps, which is required to produce a sufficiently steady output in combination with the delayed outlet switching. Finally, a GSR reactor cluster of 10 reactors (diameter = 1.23 m, height = 3.69 m) is considered. The chosen reactor diameter will operate the reactor in the bubbling fluidization regime with fluidization velocities of around 0.4 m/s when a conventional particle size of 150 μm is used.

Fig. 5a shows a cycle of the GSR reactor. In the reduction step (0–1 on the x-axis), the PSA off-gas is combusted to CO_2 and H_2O, reducing the oxygen carrier. Subsequently, in the reforming step (1–4 on the x-axis), the methane is reformed to syngas. Since the reforming reactions are highly endothermic, the reactor temperature falls rapidly in the reforming step. Finally, in the oxidation step (4–5 on the x-axis), the oxygen carrier is oxidised by air, rapidly heating the reactor again. The undesired mixing between the steps can also be seen in Fig. 5. The primary consequences of the mixing are that 1) CO_2 from the reforming step mixes into the oxidation step outlet stream, reducing the CO_2 capture efficiency, and 2) N_2 from the oxidation step mixes into the reduction step outlet stream, reducing the CO_2 purity.

Fig. 5 also compares the two most efficient cases (namely case 3 and 4 in section Improvements in design of GSR-H2 process) considered in the present study: those with added thermal mass in the reactor and with a two-phase heat exchanger in the process configuration. The difference

Please cite this article as: Nazir SM et al., Pathways to low-cost clean hydrogen production with gas switching reforming, International Journal of Hydrogen Energy, https://doi.org/10.1016/j.ijhydene.2020.01.234

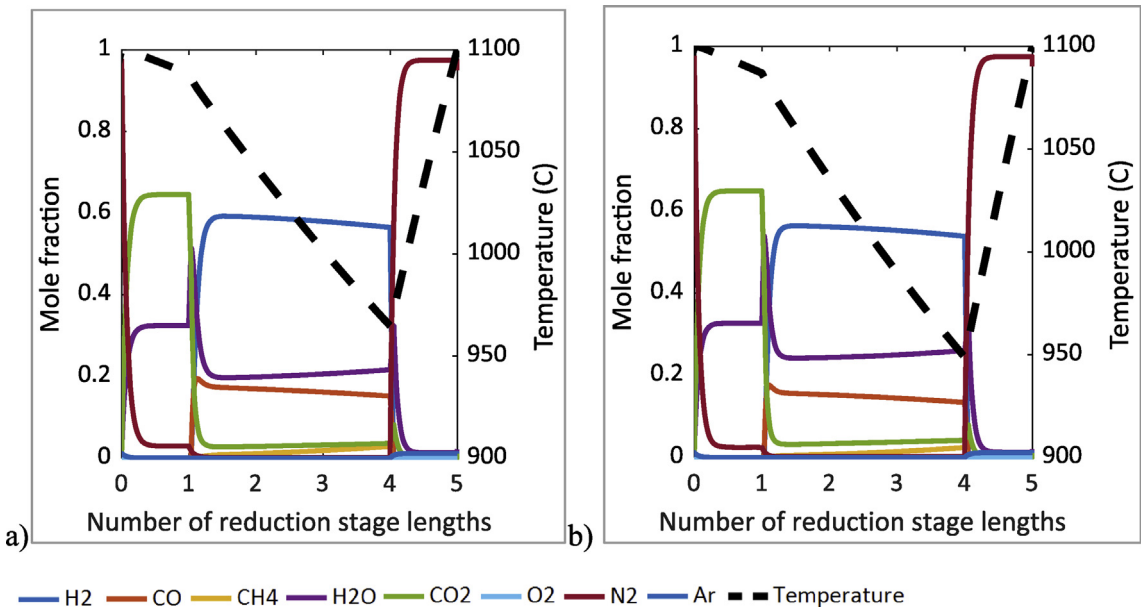

Fig. 5 – The temperature and composition as a function of the number of reduction step lengths for a full cycle of the GSR for a) without and b) with air preheating. The reduction step lengths are 101 s and 79 s respectively. Both cases consider the reactor with added thermal mass and the plant configuration with a two-phase heat exchanger.

between the two panels is that for the case in panel b) the air stream is pre-heated before entering the reactor. This slightly increases the temperature fluctuation over the cycles, since less energy is required to heat the incoming air, causing a greater temperature increase in the oxidation step for the same oxygen carrier utilization.

It can be noted that a previous study [17] already showed that adding additional thermal mass to the reactor leads to a large reduction in the temperature variation across the cycle. This results in a higher average reactor temperature in the reforming step, which leads to a higher methane conversion. Furthermore, it can be noted that adding the two-phase heat exchanger to the process configuration had a negligible effect on the reactor cycle, therefore the results for cases without the two-phase heat exchanger are not shown here.

Process model for SMR and GSR-H2

The SMR and GSR-H2 process are simulated and analysed using Aspen Hysys V8.6 [31]. Peng-Robinson thermodynamic model is used to estimate the properties of components and mixtures at equilibrium. The components in the process including heat exchangers, boilers, reactors, compressors and expanders are modelled as per the assumptions used in Nazir et al. [17]. The PSA has been modelled as a black box and the recovery of 99.999% pure H_2 is estimated using Eq. (8) [17], where P_1 and P_2 are the pressure of the PSA inlet and off-gas stream respectively. One natural draft cooling tower is considered for each process, in which the cooling water temperature rise is assumed to be 12 °C.

$$H_2 \text{ recovery in PSA } (\%) = 100 - \frac{100}{0.2521\left(\frac{P_1}{P_2}\right) + 1.2706} \quad (8)$$

Methodology for techno-economic analysis

Techno-economic analysis deals with assessment of potential of a technology in early stages of its development. The main key performance indicators to assess and compare hydrogen production processes are hydrogen production efficiency, equivalent hydrogen production efficiency, CO_2 capture and avoidance, specific primary energy consumption for CO_2 avoided (SPECCA), and economic indicators of levelised cost of hydrogen (LCOH) and cost of CO_2 avoidance (COCA). The method to estimate these key performance indicators is described below and is divided in two sections: process analysis methodology and economic analysis methodology. The basis for analysis is 10 TPH NG input to the process.

Process analysis methodology

Firstly, equivalent NG ($m_{eq,NG}$) is calculated using Eq. (9) that accounts not only for the NG consumed in the process but also for steam exports from the process and the net electrical work. Q_{th}, as calculated in Eq. (10), is the amount of energy available in the steam exported and it is divided by a factor of 0.9 in Eq. (9) to account for the use of NG to prepare the same amount of steam in a boiler. W_{el} is the net electrical work consumed in the process and is divided by a factor of 0.583 that accounts for the use of NG used to produce the same amount of electricity in a NGCC plant [32].

$$\dot{m}_{eq,NG} = \dot{m}_{NG} \times LHV_{NG} - \frac{Q_{th}}{0.9} - \frac{W_{el}}{0.583} \quad (9)$$

$$Q_{th} = \dot{m}_{steam\ export} \times \left(h_{steam@6bar} - h_{liqsat@6bar}\right) \quad (10)$$

The hydrogen production efficiency (η_{H_2}) and the equivalent hydrogen production efficiency (η_{eq,H_2}) are calculated using Eq. (11) and Eq. (12).

$$\eta_{H_2} = \frac{100\% \times \dot{m}_{H2} \times LHV_{H_2}}{\dot{m}_{NG} \times LHV_{NG}} \quad (11)$$

$$\eta_{eq,H_2} = \frac{100\% \times \dot{m}_{H2} \times LHV_{H_2}}{\dot{m}_{eq,NG} \times LHV_{NG}} \quad (12)$$

The amount of CO_2 captured (CC) and CO_2 avoided (CA) is calculated using Eq. (13) and Eq. (14). The CO_2 emission intensities of NG combustion (E_{NG} = 56.8 g_{CO2}/MJ_{LHV}), steam generation (E_{th} = 63.3 g_{CO2}/MJ) and electrical work consumed (E_{el} = 97.7 g_{CO2}/MJ) are used to calculate the CO_2 avoided from the process. The values of E_{th} and E_{el} will change if the factor for energy conversion of NG into steam (0.9 as in Eq. (9)) and electricity (0.583 as in Eq. (9)) is changed.

$$CC = \frac{100\% \times mass\ of\ CO_2\ captured}{\dot{m}_{NG} \times LHV_{NG} \times E_{NG}} \quad (13)$$

$$CA = \frac{100\% \times mass\ of\ CO_2\ captured}{\dot{m}_{NG} \times LHV_{NG} \times E_{NG} - Q_{th} \times E_{th} - W_{el} \times E_{el}} \quad (14)$$

The CO_2 emission intensity of the process and its equivalent in terms of g_{CO2}/MJ is calculated using Eq. (15) and Eq. (16), whereas the SPECCA is calculated using Eq. (17).

$$E_{CO2} = \frac{mass\ of\ CO_2\ emitted}{\dot{m}_{H2} \times LHV_{H2}} \quad (15)$$

$$E_{eq,CO_2} = \frac{mass\ of\ CO_2\ emitted\ - Q_{th} \times E_{th} - W_{el} \times E_{el}}{\dot{m}_{H2} \times LHV_{H2}} \quad (16)$$

$$SPECCA = 1000 \times \frac{\frac{1}{\eta_{eq,H2}} - \frac{1}{\eta_{eq,H2,ref}}}{E_{eq,CO2,ref} - E_{eq,CO2}} \quad (17)$$

Economic analysis methodology

The economic analysis for the GSR-H2 process and its comparison with the conventional SMR technology is carried out in accordance to the methodology proposed by the Global CCS Institute [33]. LCOH is calculated using Eq. (18).

$$LCOH = \frac{(TCR)(FCF) + FOM}{(\dot{m}_{H2})(CF*8766)} + VOM + (FC)(HR) \quad (18)$$

The definition of the terms used in Eq. (18) is presented in Table 1. The fixed charge factor (FCF) is calculated using Eq. (19) that converts the total capital value into uniform annual amounts. The FCF is a function of discount rate and lifetime of the plant. In this study a discount rate of 10% and lifetime of 30 years have been assumed.

$$FCF = \frac{r(1+r)^T}{(1+r)^T - 1} \quad (19)$$

The total capital requirement (TCR) for the process is estimated using the method described in Table 2 based on the bare erected cost (BEC) of the equipment defined as the sum of the installed cost of the equipment. The costs have been adjusted to the year 2019 costs using chemical engineering plant cost index (CEPCI) factors [34]. The installed costs for heat exchangers, boilers, air compressors and N_2-turbine is taken from the databases available in the economics tool in ASPEN Hysys V8.6 [31] and the PEACE component of the Thermoflow suite V26 [35]. The reference costs for desulphurization unit, pre-reformer, FTR, WGS reactor, PSA and hydrogen compressors are referred from Spallina et al. [5]. The installed costs for PSA off-gas compressor, CO_2 compression step and steam turbines is referred from Szima et al. [27]. GSR reactor costs are also estimated using the same methodology as presented in Szima et al. [27] using cost correlations from Turton et al. [36]. In the cases with added thermal mass, stainless steel rods were included in the reactor cost using a purchase price of 1725 $/ton, based on an online search. The purchase cost was tripled to estimate installed costs, which is similar to the practice employed in Turton et al. [36].

A process contingency of 30% is assumed for the GSR reactor since this reactor concept has been demonstrated on lab scale [23,37] and is being proposed for pilot scale demonstration. Process contingencies for all the other sections of the GSR-H2 plant and the reference plant is 0% since the process technology is already in commercial use. The project contingency is assumed 10% [33] for both the processes since a complete process and engineering design can be easily developed during the project phase. Owner's costs may include land and financing costs, inventory capital and start-up costs and accounts for

Table 1 – Definition of terms in Eq. (18) to calculate the levelised cost of hydrogen (LCOH).

Parameter	Definition	Unit
TCR	Total Capital Requirement in the base year of the analysis	$
FCF	Fixed Charge Factor as defined in Eq. 19	fraction
FOM	Fixed O&M costs	$/year
$\dot{m}_{H2}$	Mass of hydrogen produced from the process	kg/hr
CF	Capacity Factor – availability of the plant	Fraction
VOM	Variable O&M costs excluding the fuel costs	$/kg-$H_2$
HR	Net heat rate of the plant	MJ/kg-H_2
FC	Fuel Cost per unit of energy	$/MJ
r	Interest or discount rate	%
T	Economic lifetime of the plant relative to its base year	years

Table 2 – Methodology and assumptions to estimate the total capital requirement (TCR).

Component	Definition
Bare Erected Cost (BEC)	Sum of installed cost of equipment
Engineering Procurement Construction Costs (EPCC)	8% of BEC
Process Contingency	30% of BEC for GSR reactor; 0% for reference SMR plant and for remainder of the GSR-H2 process
Project Contingency	10% of (BEC + EPCC + Process Contingency)
Total Contingencies	Process Contingency + Project Contingency
Total Plant Costs (TPC)	BEC + EPCC + Total Contingencies
Owner's Cost	20.2% of TPC [38]
Total Overnight Costs (TOC)	TPC + Owners Cost
Total Capital Requirement (TCR)	1.14*TOC [38]

Please cite this article as: Nazir SM et al., Pathways to low-cost clean hydrogen production with gas switching reforming, International Journal of Hydrogen Energy, https://doi.org/10.1016/j.ijhydene.2020.01.234

20.2% of the total plant cost (TPC) in power plants as reported in the cost methodology adopted by DOE/NETL [38]. Similar owner's cost is assumed in this study. The total overnight cost (TOC), which is the sum of TPC and owner's cost, is multiplied by a factor of 1.14 to obtain the TCR. The factor 1.14 represents the increase in capital due to both escalation and interest during construction of an investor owned utility [38].

The assumptions used to estimate the fixed (FOM) and variable (VOM) operating and maintenance costs are listed in Table 3. To calculate the labour costs, 3 working shifts with 12 people in each are considered for the reference plant. Additional 3 people per shift are considered for the CO_2 compression section in the GSR-H2 plant with CO_2 capture. The NG price is assumed to be 6.9 $/GJ-LHV, but this is region and time specific, as is the electricity price. A sensitivity study for different NG and electricity price is presented in the results and discussion section. All the other assumptions listed in Table 3 are similar to previous studies [5,26] except that the euro to US dollar currency conversion rate is assumed to be 1.15 USD/EUR.

After calculating the LCOH of the processes, the cost of CO_2 avoided (COCA) is calculated using Eq. (20). The difference between the LCOH of the GSR and reference plants is divided by difference in specific CO_2 emissions in the plants to calculate the COCA. Although the LCOH will generally be reported including the CO_2 tax shown in Table 3, the COCA reported in Table 4 is calculated using LCOH numbers without any CO_2 tax. Therefore, the value of COCA also gives the minimum CO_2 emissions tax value needed to make the GSR-H2 process economically more attractive than the conventional SMR plant.

Table 3 – Assumptions for fixed and variable operating and maintenance costs and fuel costs.

Fixed O&M Costs		
Operating Labor	60,000	$/person-year
Maintenance, Support and Administrative Labor	2.5	% of TOC
Property Taxes	Included in $6#insurance costs	
Insurance costs	2	% of TOC
NG price (Fuel Cost)	6.9	$/GJ LHV
Variable O&M Costs		
Consumables		
Cooling Water Make Up Costs	0.4	$/m^3
Process Water Cost	2.3	$/m^3
Catalysts and Sorbent Replacement		
Oxygen Carrier cost	15	$/kg
WGS catalyst cost	16,100	$/m^3
Adsorbent cost $6#(mixture of activated $6#carbon and Zeolite 5A)	1.1	$/kg [39,40]
Replacement Period	5	Years
CO_2 Transport and $6#Storage Costs	11.5	$/ton CO_2
Emissions Tax (CO_2 tax)	23	$/ton CO_2
Electricity price	69	$/MWh
Steam exports	2.1	$/ton [41]

$$COCA\left(\frac{\$}{ton_{CO2}}\right) = \frac{LCOH_{GSR-H2} - LCOH_{ref}}{\left(\frac{\dot{m}_{CO2}}{\dot{m}_{H2}}\right)_{ref} - \left(\frac{\dot{m}_{CO2}}{\dot{m}_{H2}}\right)_{GSR-H2}} \quad (20)$$

Results and discussions

This section is presented in three parts. The first two parts describe the technical and economic performance of the different GSR-H2 process configurations compared to the SMR benchmark. The third part consolidates the discussion in the first two sub-sections and presents scenarios, challenges and opportunities for deployment of GSR-H2 process in the form of different sensitivity studies. The main results for the techno-economic analysis for the SMR and GSR-H2 processes are presented in Table 4.

Technical analysis

The detailed technical performance comparison between the conventional SMR plant and the base case GSR-H2 process with and without added thermal mass was reported in Nazir et al. [17]. Results in this section are more focussed towards improvements in the GSR-H2 process. The conditions in the GSR-H2 process for different cases are shown in Table 5.

Effect of having a two-phase evaporator (GSR-H2 in case 2)
Case 2 has 0.93%-point higher equivalent hydrogen production efficiency than the base case GSR-H2 process. In case 2, low temperature heat is utilised in preparing steam in the two-phase evaporator, resulting in lower heat rejection to the cooling water as seen in Table 5. This slightly improved heat recovery allowed for 25 °C greater pre-heating of the fuel and steam to reforming, requiring a little less PSA off-gas combustion to heat the inlet gases in the GSR. This is reflected in a lower air (oxygen) requirement and a 0.35 %-point higher hydrogen production efficiency. Table 5 also shows a higher S/C ratio for this case. This is the result of a lower PSA off-gas requirement that demands more H_2 extraction from the syngas which, in turn, requires more steam to increase CH_4 conversion in the GSR reactors and CO conversion in the WGS reactors. The reforming step is also slightly longer, leading to a lower average reforming temperature, which requires more steam to increase CH_4 conversion. The net electricity consumption in case 2 is 6.6% lower than in base case, mainly due to lower compression work for compressing air (lower air flow to GSR), hydrogen (lesser pressure drop in the syngas stream due to the absence of NG pre-heater), PSA off-gas (lower PSA off-gas demand) and CO_2 stream (using two-phase evaporator cools down the CO_2 stream in one step, avoiding higher pressure drops due to multiple coolers as in the base case and case 1). Since a fraction of steam is prepared in the two-phase evaporator in case 2, the heat in N_2 stream can be used in the N_2-turbine to produce more power when compared to the base case. Therefore, integrating the two-phase evaporator in the GSR-H2 process to raise steam for reforming reduces the efficiency penalty in GSR-H2 process

Please cite this article as: Nazir SM et al., Pathways to low-cost clean hydrogen production with gas switching reforming, International Journal of Hydrogen Energy, https://doi.org/10.1016/j.ijhydene.2020.01.234

Table 4 – Main results for techno-economic analysis.

Cases	Units	SMR	GSR-H2				
			Base case	Case 1	Case 2	Case 3	Case 4
Technical analysis							
$m_{eq,NG}$	TPH	9.83	11.402	10.76	11.31	10.80	11.41
Steam to Carbon ratio		2.70	2.66	1.80	2.90	1.85	2.19
H_2 produced	TPH	3.02	3.33	3.30	3.35	3.36	3.52
Hydrogen production efficiency	%	77.92	86.03	85.00	86.38	86.78	90.73
Equivalent H_2 production efficiency	%	79.28	75.45	79.01	76.38	80.37	79.50
Electricity Consumed							
Air compressor/blower	MW	0.33	6.78	6.98	6.48	6.55	5.83
H_2 compressors	MW	2.58	2.90	2.86	2.87	2.88	3.01
Pumps	MW	0.13	0.06	0.04	0.06	0.04	0.05
Off-gas compressor	MW		4.41	4.56	4.35	4.49	4.46
CO_2 compression	MW		0.87	0.81	0.72	0.73	0.71
Electricity Produced							
Steam Turbine	MW	2.61	–	–	–	–	–
N_2-turbine	MW		4.46	8.52	4.62	7.77	3.42
Net Electric Power	MW	−0.43	−10.56	−6.73	−9.86	−6.92	−10.64
Steam Exported (6 bar)	TPH	4.52	0.00	2.70	0.00	2.39	0.00
Q_{th}	MJ/hr	9592	0	5702	0	5044	0
Specific CO_2 emissions	g-CO_2/MJ	72.90	2.12	2.00	1.99	1.83	1.66
Equivalent specific CO_2 emissions	g-CO_2/MJ	71.64	11.40	7.07	10.62	7.07	10.53
SPECCA	MJ/kg-CO_2		1.06	0.07	0.79	−0.26	−0.06
CO_2 capture	%		96.21	96.57	95.43	96.15	96.46
CO_2 avoidance	%		84.35	89.75	84.36	89.03	84.50
Economic analysis							
Capital costs	\$/kg-H_2	0.40	0.38	0.42	0.39	0.42	0.38
VOM	\$/kg-H_2	0.24	0.35	0.26	0.33	0.26	0.32
FOM	\$/kg-H_2	0.22	0.22	0.23	0.22	0.23	0.22
Fuel costs	\$/kg-H_2	1.06	0.96	0.97	0.96	0.95	0.91
LCOH	\$/kg-H_2 (considering no emission tax)	1.92 (1.71)	1.91 (1.91)	1.88 (1.88)	1.90 (1.89)	1.86 (1.85)	1.83 (1.82)
COCA	\$/t-CO_2	–	26.39	21.16	24.01	18.03	15.00

from 3.8%-points to 2.9%-points with reference to the conventional SMR plant, reducing the SPECCA from 1.06 to 0.79 MJ/kg-CO_2.

Effect of additional thermal mass and two-phase evaporator (GSR-H2 in case 3)

Having additional thermal mass in the GSR results in overall higher temperatures in the reactor. This allows the required fuel conversion to be achieved with a lower S/C ratio, leading to considerably less rejection of the condensation enthalpy of excess steam in the syngas to the cooling water as seen in Table 5. The main benefit of the lower steam requirement is that the N_2 stream can be expanded from a high TIT, leading to 74% greater power production from the N_2-turbine compared to case 2. Additional heat after the N_2-turbine is exported as 6 bar steam. This reduction in electricity consumption and increase in steam exports increase the equivalent hydrogen production efficiency of case 3 by 3.99 %-points relative to case 2, even though hydrogen production efficiency is only 0.4 %-points higher. This makes case 3 more efficient than the SMR benchmark, resulting in a negative SPECCA value of −0.26 MJ/kg-CO_2.

Table 5 – Conditions in the GSR-H2 process.

Cases	GSR-H2				
	Base case	Case 1	Case 2	Case 3	Case 4
Steam to carbon (S/C) ratio	2.66	1.80	2.90	1.85	2.19
Reforming inlet Temperature (°C)	825	900	850	980	980
Syngas temperature (°C)	939	1027	927	1021	1012
CH_4 mol% in syngas	2.12	1.46	2.09	1.50	1.17
WGS inlet temperature (°C)	302	331	299	289	269
Reduction step outlet temperature (°C)	1080	1095	1078	1094	1093
Oxidation step outlet temperature (°C)	990	1045	983	1040	1033
TIT for N_2-turbine (°C)	456	1045	505	1015	384
Air flowrate to GSR (TPH)	45.5	46.9	43.5	43.9	39.0
Heat rejection to cooling water (MW)	19.6	14.5	17.2	12.3	13.3

Effect of heat integration with pre-heated air for oxidation step of the GSR (case 4)

Pre-heating air for the oxidation step of the GSR with the N_2 stream reduces the amount of PSA off-gas combustion required to heat the air stream to the reactor temperature. This allows more of the heating value in the fuel to be converted to H_2 instead of heat and is reflected in a 3.95 %-point increase in hydrogen production efficiency compared to case 3. However, the lower PSA off-gas requirement needs greater H_2 extraction in the PSA unit, which requires more steam for converting CH_4 and CO to H_2, hence the increase in S/C ratio relative to case 3. The main trade-off for the increased

Please cite this article as: Nazir SM et al., Pathways to low-cost clean hydrogen production with gas switching reforming, International Journal of Hydrogen Energy, https://doi.org/10.1016/j.ijhydene.2020.01.234

hydrogen production efficiency is the low N_2-turbine inlet temperature (TIT) that strongly reduces power production relative to case 3. Hence, case 4 increases H_2 production at the cost of greater net electricity consumption. Relative to case 3, this configuration loses 0.87 %-points of equivalent H_2 production efficiency, but this is only due to the absence of 6-bar steam exports with limited economic value.

Economic analysis

Table 4 and Fig. 6 present the main results from the economic analysis of the SMR and GSR-H2 processes. Fuel cost accounts for the maximum share in the LCOH in both the processes, with 55% of the LCOH in SMR plant and 49–52% of the LCOH in GSR-H2 cases. The fuel cost element in the LCOH is inversely proportional to the hydrogen production efficiency. In the SMR plant, the capital requirement contributes about 21% of the LCOH and is in a similar range (20–21%) for GSR-H2 cases that have N_2 turbines with lower TITs (base case, case 2 and 4). In case 1 and 3, higher N_2 turbine power output results in higher turbo-machinery costs as shown in Fig. 7a. The costs associated with heat exchangers is higher in SMR plant because of the lower heat transfer coefficient for gas-gas heat transfer in the pre-heaters that recover heat from the low-pressure exhaust gas from the FTR burners. Case 4 of GSR-H2 has an additional air pre-heater before the oxidation step of the GSR resulting in higher heat exchanger related capital costs when compared to other GSR-H2 cases. However, the costs associated with high temperature turbomachinery is relatively high and, therefore, the capital cost element in LCOH for case 1 and 3 is 1–2 %-points higher than the other GSR cases. Fig. 7a also shows that the GSR reactors have a slightly lower cost than the FTR unit in the SMR benchmark case, even after adding a 30% process contingency to GSR. This is due to the simplicity of the GSR reactors relative to the FTR that houses a large number of pressurized reforming tubes in a high temperature furnace. The FOM cost is higher in case 1 and 3 because these costs are calculated as a fixed fraction of capital costs.

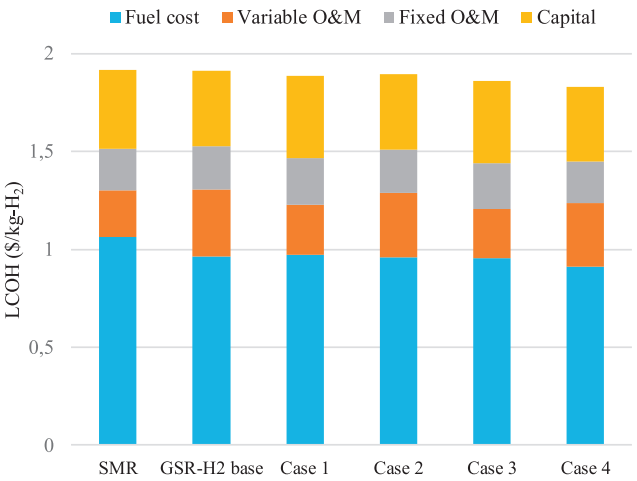

Fig. 6 – Distribution of different components of levelised cost of hydrogen (LCOH) for SMR and GSR-H2 process.

The VOM costs in the SMR plant account for 12.4% of the LCOH, whereas it ranges between 13 and 18% for the GSR-H2 process. The VOM costs in the SMR plant are mainly associated with the emission taxes, whereas electricity and CO_2 transport and storage costs account for the major fraction of the VOM costs in GSR-H2 process (Fig. 7b). The CO_2 transport and storage costs are similar in all the GSR-H2 cases since the CO_2 capture rate is similar. However, the VOM costs for cases with higher electrical demand are higher.

For the assumptions described in section Economic analysis methodology, the base case GSR-H2 plant with ~96% CO_2 capture has a slightly lower LCOH when compared to SMR plant without CO_2 capture. The VOM costs in the base case GSR-H2 process are higher due to higher net electricity demand, which is compensated by higher hydrogen production efficiency and hence lower fuel costs than the SMR plant. The improvements in cases 1–4 help in reducing the hydrogen production costs from the GSR-H2 process. Case 4 has the lowest LCOH which is ~4.5% less than the LCOH from SMR plant. Case 3 has the highest equivalent hydrogen production efficiency but has 1.6% higher LCOH than the GSR-H2 process in case 4, because case 4 produces more hydrogen at the cost of higher overall electricity input. Although the CO_2 emission tax of 23 $/t-$CO_2$ was assumed to calculate the LCOH, it is shown in Table 4 that an emission tax value of 15 $/t-$CO_2$ will make the GSR-H2 process configured according to case 4 economically more attractive than the SMR plant.

Most components of the GSR-H2 process are technologically mature, implying that uncertainties involved in capital cost estimation using the established commercial tools employed in this study are relatively small. In addition, the GSR-H2 plants use a process layout with similar process components to the benchmark SMR plant, so any uncertainties in the costs of components like the pre-reformer, water-gas shift reactors and PSA unit will have a limited effect on conclusions from this comparative study. The only process component at a lower technology readiness level is the GSR reactor. In this case, uncertainty is limited by the simplicity of the standalone bubbling fluidized beds employed, so the capital cost estimate with the 30% added process contingency should be reasonable. However, the long-term stability of the oxygen carrier serving to combust the fuel and catalyse the reforming reactions presents an important technical uncertainty. Fig. 8 shows the effect of oxygen carrier lifetime on the LCOH from GSR-H2 processes. For oxygen carriers having a lifetime between 3 months and 5 years, the LCOH varies between 4 and 5%. Increasing the oxygen carrier lifetime beyond 1 year improves the LCOH by less than 1%, but shorter lifetimes than 1 year start to have significant adverse effects on competitiveness. Therefore, demonstrating oxygen carriers with high mechanical strength and thermochemical stability over many redox cycles is critical for deployment of GSR technology for clean hydrogen production.

Alongside the uncertainty in oxygen carrier stability, there is uncertainty associated with the other O&M cost elements like NG and electricity price and CO_2 tax. The effect of these cost elements on the LCOH is discussed in the next section. The uncertainty associated with catalyst and adsorbent costs is less as these have been in commercial use. Uncertainty

Please cite this article as: Nazir SM et al., Pathways to low-cost clean hydrogen production with gas switching reforming, International Journal of Hydrogen Energy, https://doi.org/10.1016/j.ijhydene.2020.01.234

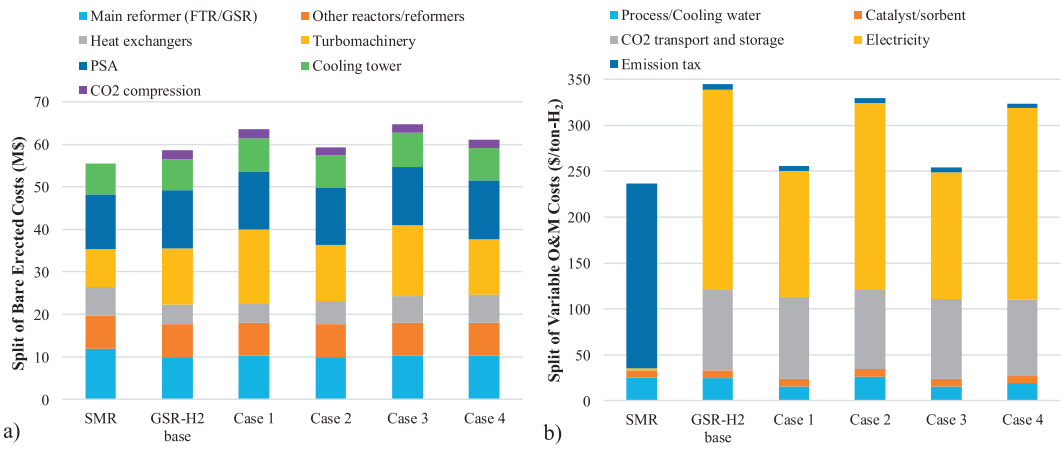

Fig. 7 – Split of the a) Bare erected cost b) Variable O&M costs.

associated with steam exports have minimal impact on the LCOH of the processes.

Finally, an important technical uncertainty that should be mentioned is the performance and durability of high temperature valves downstream of the GSR reactor. If technical constraints from these valves restrict the maximum reactor temperature below the value of 1100 °C assumed in this study, the efficiency of the process will decline as more steam will be needed to achieve sufficient fuel conversion, increasing fuel consumption and cost. On the other hand, valves that can operate at even higher temperature could further improve GSR efficiency. This is an important element that must be demonstrated during scale-up of the GSR technology.

Scenarios for low-cost hydrogen production with CO_2 capture using GSR

As discussed in the previous section, fuel cost is the major component of the LCOH in both the SMR and GSR-H2 plants. GSR-H2 processes shift some of this energy input to electricity, making the electricity price another important parameter. In addition, CO_2 transport and storage costs are also uncertain with CO_2 utilization potentially resulting in low or negative costs, whereas public resistance and insufficient scale can strongly increase costs. Fig. 9 therefore shows the sensitivity of the LCOH and COCA of SMR and GSR-H2 plants to NG price, electricity price and CO_2 transport and storage costs. The COCA presented in Fig. 9 is equivalent to the minimum CO_2 emission tax needed to make the GSR-H2 process more economically attractive than the SMR plant.

The SMR and GSR-H2 processes are highly sensitive to the NG price as seen in Fig. 9a. From the reference price of NG (6.9 $/GJ-LHV), a change in NG price by 2 $/GJ-LHV affects the LCOH in SMR plant by 16% and in the GSR-H2 plant by 14–15%. Since the GSR plants displace some NG energy input with electricity, they are less sensitive to increases in NG price. This also explains the reduction in COCA as NG price is increased (Fig. 9b). At a very high NG price of 9 $/GJ-LHV, the GSR-H2 (case 4) process will need only a CO_2 emission tax of 8 $/t-$CO_2$ for the GSR-H2 process with >96% CO_2 capture to perform economically better than the SMR plant without capture.

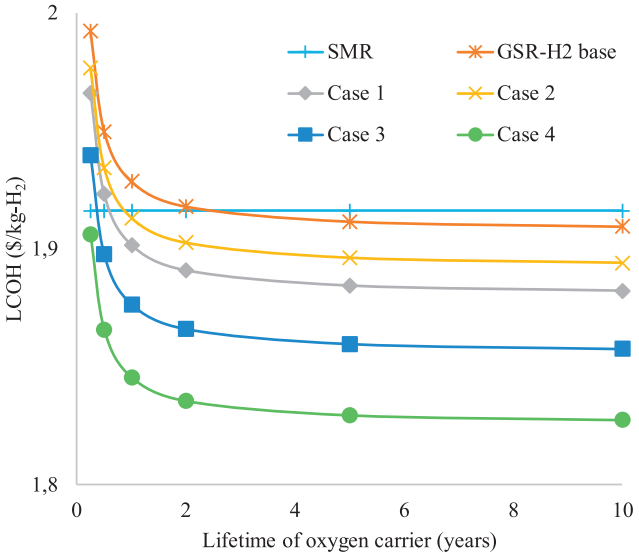

Fig. 8 – Effect of oxygen carrier lifetime on levelised cost of hydrogen from GSR-H2 process.

Fig. 9c shows the sensitivity of the LCOH of SMR and GSR-H2 plants with change in electricity price. The low power consumption of the SMR plant makes it insensitive to the electricity price. However, the LCOH of the GSR-H2 plant varies between 2 and 4% when electricity price changes by 20 $/MWh around the base value of 69 $/MWh. This difference in sensitivity is best exemplified by comparing cases 3 and 4. The trade of more H_2 production for greater electricity consumption in case 4 makes it more sensitive to electricity price variations. As expected, Fig. 9d shows that higher electricity prices substantially increase the COCA for all GSR plants. Although not directly studied here, it can be noted that COCA will also vary with the source of electricity, which influences the indirect CO_2 emissions of the GSR plant. The effect of electricity source on the CO_2 avoidance rate was discussed in Nazir et al. [17]. In general, GSR will be most attractive when clean electricity can be bought from the grid at a low cost. This should be an important consideration when considering investment in GSR-H2 plants.

Please cite this article as: Nazir SM et al., Pathways to low-cost clean hydrogen production with gas switching reforming, International Journal of Hydrogen Energy, https://doi.org/10.1016/j.ijhydene.2020.01.234

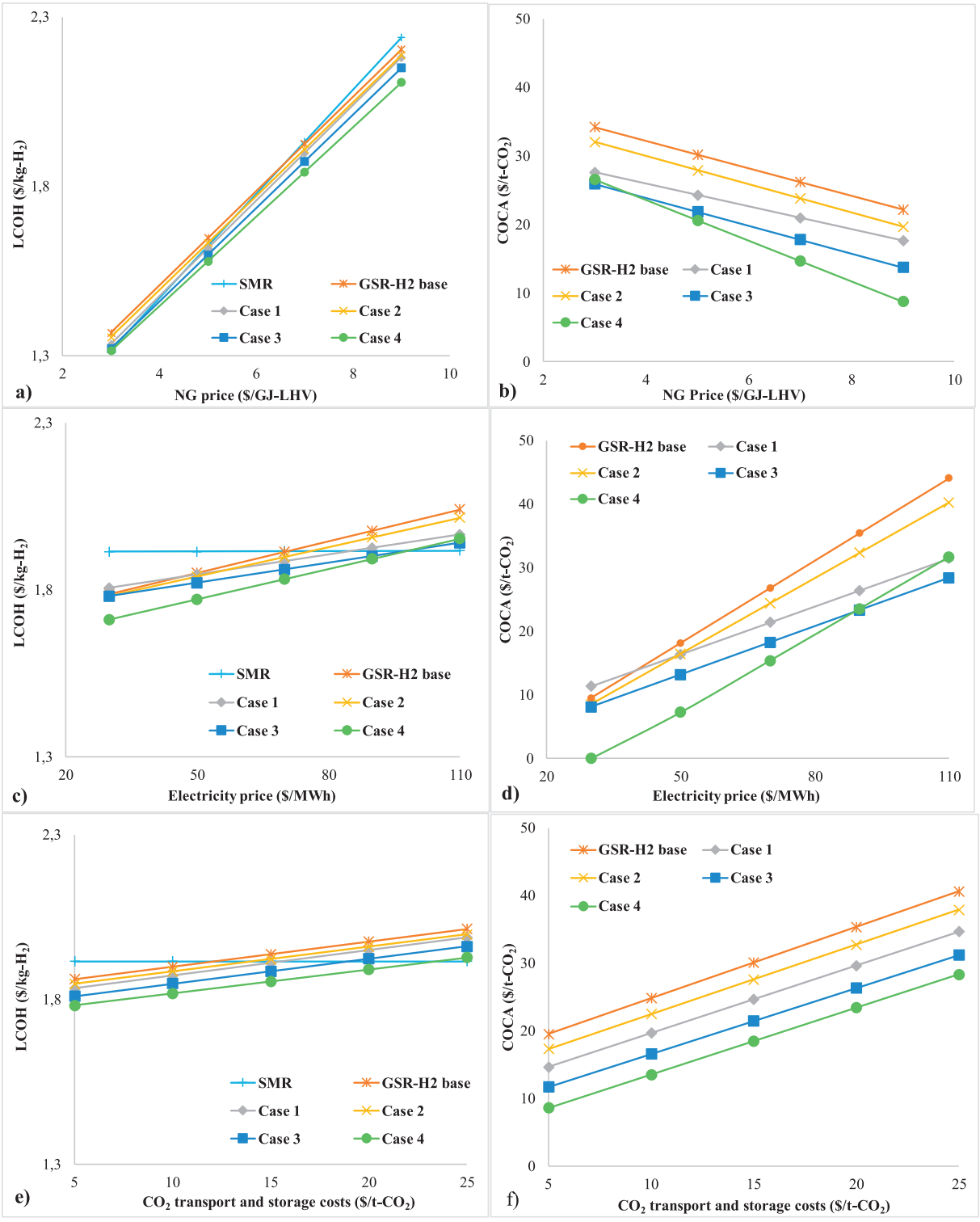

Fig. 9 – Sensitivity studies a) NG price vs LCOH b) NG price vs COCA c) Electricity price vs LCOH d) Electricity price vs COCA e) CO_2 transport and storage costs vs LCOH f) CO_2 transport and storage costs vs COCA.

The CO_2 transport and storage costs depend on the type of transport and also the scale of flow being transported [42]. Fig. 9e shows the sensitivity of the LCOH of GSR-H2 plants with the CO_2 transport and storage costs. If the transport and storage costs are doubled, the LCOH of the GSR-H2 processes increases by 4%. Naturally, COCA increases in direct proportion with the CO_2 transport and storage cost (Fig. 9f).

When considering the range of COCA values in Fig. 9, it is clear that all three of these variables have a significant impact on the competitiveness of GSR-H2 against conventional SMR. However, over the ranges investigated, the electricity price

Please cite this article as: Nazir SM et al., Pathways to low-cost clean hydrogen production with gas switching reforming, International Journal of Hydrogen Energy, https://doi.org/10.1016/j.ijhydene.2020.01.234

Table 6 – Definition of scenarios with different NG and electricity price and CO_2 emission tax.

Scenarios	NG price ($/GJ-LHV)	Electricity price ($/MWh)	Emission tax ($/t-$CO_2$)
1	3	30	0
2	3	30	25
3	3	30	50
4	9	30	0
5	9	30	25
6	9	30	50
7	3	90	0
8	3	90	25
9	3	90	50
10	9	90	0
11	9	90	25
12	9	90	50

has the largest impact, with the natural gas price and CO_2 transport and storage costs showing a slightly lower sensitivity.

Fig. 9 showed the sensitivity of the LCOH and COCA of SMR and GSR-H2 plants with the important future energy market drivers like NG price, electricity price and CO_2 transport and storage costs. However, the future energy scenario is complex and will depend on multiple factor interaction. Table 6 presents twelve different future energy scenarios that reflect the change in NG price, electricity price and stricter emission regulations through a CO_2 tax. The NG price is location dependent, for example ~3 $/GJ-LHV in USA and 6–8 $/GJ-LHV in Europe [43] and is projected to increase in the future energy scenarios [28,44]. The electricity price from thermal plants is sensitive to the fuel price, and with CCS increases the price by 15–30% [44]. However, the electricity generation sector is undergoing a major shift towards renewables. This shift has brought down the cost of electricity from renewables drastically in the last 10 years [45]. Clean energy transitions also depend on policy measures to control emissions. For example, the CO_2 emission tax is projected to increase with stricter guidelines for industries to reduce their emissions. Scenarios 1–3 and 7–9 in Table 6 depict scenarios with low NG price (for example: USA and the Middle East), with scenarios 1–3 having low electricity price (for example: countries with abundant local fossil fuel reserves like the Middle East and/or renewable energy potential like Norway) and scenarios 7–9 having high electricity prices (for example: fossil fuel importers with limited renewable energy potential like Japan). The scenarios also show the effect of increasing CO_2 emission taxes. Scenarios 4–6 and 10–12 depict scenarios with high NG price (for example: NG importers like Europe, Japan and most of developing Asia) factoring in low and high electricity price and CO_2 emission tax.

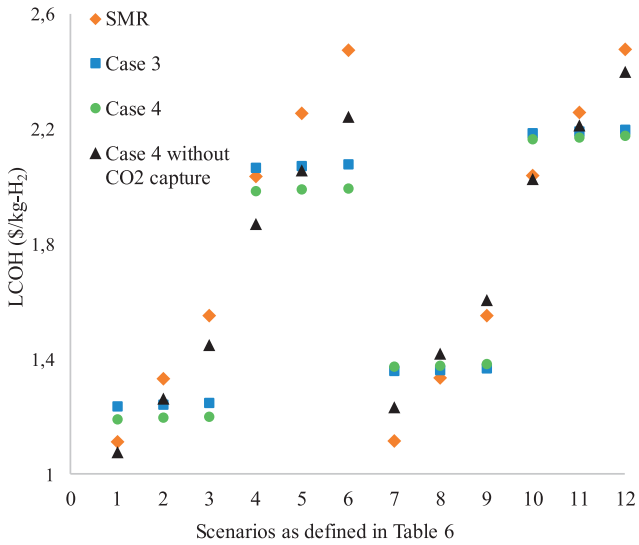

Fig. 10 – Levelised cost of hydrogen comparison for scenarios defined in Table 6.

The LCOH from the SMR benchmark and the two most promising GSR-H2 configurations (cases 3 and 4) is calculated for the twelve scenarios (Table 6) and shown in Fig. 10. Fig. 10 also shows the LCOH for an additional case: case 4 without CO_2 capture. As outlined in Nazir et al. [17], this is a promising commercialization pathway for the GSR technology. Constructing the plant without CO_2 capture can outcompete current SMR technology in an environment without significant CO_2 taxes and such a plant will be very simple to retrofit for CO_2 capture at a later stage when CO_2 taxes are higher and CO_2 transport and storage infrastructure is in place.

Fig. 10 clearly shows that case 4, either with or without CO_2 capture, is the lowest cost option in all but three of the 12 scenarios. This illustrates the robustness of the GSR-H2 business case when the retrofitting pathway described above is followed. It is only in the scenarios combining low natural gas prices with high electricity prices where the relatively high electricity consumption of case 4 reduces its competitiveness. In these scenarios, the SMR plant is the cheapest at low CO_2 prices and case 3 is cheapest at high CO_2 prices. It can also be noted that such a combination of low natural gas prices and high electricity prices is unlikely to persist for extended periods because cheap natural gas will lead to a rapid expansion of low-cost electricity from natural gas combined cycle power plants (e.g. the shale revolution in the US).

Finally, it can be mentioned that successful commercialization of GSR-H2 plants on the scale investigated in this study (10 TPH of NG) can lead to widespread deployment of GSR combined cycle power plants for flexible power and hydrogen production at a scale of 100–150 TPH of NG [27]. Such flexible GSR plants can significantly reduce overall power system costs and emissions in a future scenario with high shares of wind and solar power [46].

Conclusions

This study presented a techno-economic assessment of the GSR-H2 plant for hydrogen production from natural gas reforming with inherent CO_2 capture. Improved process configurations were devised to eliminate the energy penalty of CO_2 capture and an economic assessment was completed to assess whether the high process efficiency translates into competitive hydrogen production costs.

The GSR-H2 process achieved CO_2 avoidance costs as low as 15 $/ton, making it a promising candidate for affordable clean hydrogen production. Such advanced reforming processes are generally not considered in long-term hydrogen

Please cite this article as: Nazir SM et al., Pathways to low-cost clean hydrogen production with gas switching reforming, International Journal of Hydrogen Energy, https://doi.org/10.1016/j.ijhydene.2020.01.234

pathways such as in the recent IEA "Future of Hydrogen" [4] report where CO_2 capture from steam methane reforming plants remains expensive in longer-term scenarios. It is recommended that such high-level reports acknowledge the possibility of larger long-term cost reductions for natural gas reforming with CO_2 capture similar to the current cost reduction assumptions for electrolysis.

The most attractive commercialization pathway for the GSR-H2 technology is to first construct the plant without any CO_2 capture. In this configuration, hydrogen production costs are clearly lower than that of the SMR benchmark. When CO_2 taxes eventually increase and CO_2 transport and storage infrastructure becomes available, the plant can easily and cheaply be retrofitted for CO_2 capture to ensure decades of continued profitable operation. This pathway makes the GSR-H2 plant insensitive to uncertainties in the future development of CO_2 taxation schemes.

Oxygen carrier lifetime is the key technical uncertainty that can adversely affect GSR performance. Lifetimes below 1 year start to significantly increase the hydrogen production cost. For this reason, long-term demonstration of oxygen carrier stability under realistic GSR operating conditions should be the first priority for scale-up and commercialization of this promising clean energy technology. Following this demonstration, the simplicity of the GSR reactor design can allow for rapid scale-up to commercial scale.

When considering operating costs, a distinguishing feature of GSR-H2 is that it exchanges some fuel consumption for electricity consumption. Relative to conventional SMR, this makes the GSR-H2 plant more suitable to regions with higher fuel costs and/or lower electricity prices. The trade-off between fuel and electricity consumption can be controlled with small changes to the GSR-H2 process layout to adapt the plant to application in different world regions.

Based on all these features of the GSR-H2 process, further scale-up and demonstration activities can be recommended.

Acknowledgements

The authors gratefully acknowledge the Research Council of Norway for the financial support through the ERA-NET ACT GaSTech project co-funded by the European Commission under the Horizon 2020 program, ACT Grant Agreement No. 691712. The authors also thank the project partners in GaSTech project.

REFERENCES

[1] IPCC. Climate change 2014 synthesis report: summary for policy makers. 2014.
[2] IEA. Tracking Clean energy progress, energy technology perspectives 2017 excerpt. 2017.
[3] IPCC. Summary for policymakers. In: Masson-Delmotte V, Zhai P, Pörtner H-O, Roberts D, Skea J, Shukla PR, Pirani A, Moufouma-Okia W, Péan C, Pidcock R, Connors S, Matthews JBR, Chen Y, Zhou X, Gomis MI, Lonnoy E, Maycock T, Tignor M, Waterfield T, editors. Global Warming of 1.5°C. An IPCC Special Report on the impacts of global warming of 1.5°C above pre-industrial levels and related global greenhouse gas emission pathways, in the context of strengthening the global response to the threat of climate change, sustainable development, and efforts to eradicate poverty [, vol. 32. Geneva, Switzerland: World Meteorological Organization; 2018.
[4] IEA. The future of hydrogen: seizing today's opportunities. International Energy Agency; 2019. 2019.
[5] Spallina V, Pandolfo D, Battistella A, Romano MC, Van Sint Annaland M, Gallucci F. Techno-economic assessment of membrane assisted fluidized bed reactors for pure H2 production with CO2 capture. Energy Convers Manag 2016;120:257–73.
[6] IEA. World energy outlook. International Energy Agency; 2019.
[7] Voldsund M, Jordal K, Anantharaman R. Hydrogen production with CO2 capture. Int J Hydrogen Energy 2016;41(9):4969–92.
[8] Soltani R, Rosen MA, Dincer I. Assessment of CO2 capture options from various points in steam methane reforming for hydrogen production. Int J Hydrogen Energy 2014;39(35):20266–75.
[9] Abánades A, Rubbia C, Salmieri D. Thermal cracking of methane into Hydrogen for a CO2-free utilization of natural gas. Int J Hydrogen Energy 2013;38(20):8491–6.
[10] Khojasteh Salkuyeh Y, Saville BA, MacLean HL. Techno-economic analysis and life cycle assessment of hydrogen production from natural gas using current and emerging technologies. Int J Hydrogen Energy 2017;42(30):18894–909.
[11] Martínez I, Armaroli D, Gazzani M, Romano MC. Integration of the Ca-Cu process in ammonia production plants. Ind Eng Chem Res 2017;56(9):2526–39.
[12] Tock L, Maréchal F. H2 processes with CO2 mitigation: thermo-economic modeling and process integration. Int J Hydrogen Energy 2012;37(16):11785–95.
[13] Martínez I, Romano MC, Chiesa P, Grasa G, Murillo R. Hydrogen production through sorption enhanced steam reforming of natural gas: thermodynamic plant assessment. Int J Hydrogen Energy 2013;38(35):15180–99.
[14] Riva L, Martínez I, Martini M, Gallucci F, van Sint Annaland M, Romano MC. Techno-economic analysis of the Ca-Cu process integrated in hydrogen plants with CO2 capture. Int J Hydrogen Energy 2018;43(33):15720–38.
[15] Nazir SM, Morgado JF, Bolland O, Quinta-Ferreira R, Amini S. Techno-economic assessment of chemical looping reforming of natural gas for hydrogen production and power generation with integrated CO2 capture. Int J Greenhouse Gas Control 2018;78:7–20.
[16] Kang K-S, Kim C-H, Bae K-K, Cho W-C, Kim S-H, Park C-S. Oxygen-carrier selection and thermal analysis of the chemical-looping process for hydrogen production. Int J Hydrogen Energy 2010;35(22):12246–54.
[17] Nazir SM, Cloete JH, Cloete S, Amini S. Efficient hydrogen production with CO2 capture using gas switching reforming. Energy 2019;185:372–85.
[18] Nazir S, Bolland O, Amini S. Analysis of combined cycle power plants with chemical looping reforming of natural gas and pre-combustion CO2 capture. Energies 2018;11(1):147.
[19] Noorman S, van Sint Annaland M, Kuipers H. Packed bed reactor technology for chemical-looping combustion. Ind Eng Chem Res 2007;46(12):4212–20.
[20] Spallina V, Marinello B, Gallucci F, Romano MC, Van Sint Annaland M. Chemical looping reforming in packed-bed reactors: modelling, experimental validation and large-scale reactor design. Fuel Process Technol 2017;156:156–70.
[21] Håkonsen SF, Blom R. Chemical looping combustion in a rotating bed reactor – finding optimal process conditions for prototype reactor. Environ Sci Technol 2011;45(22):9619–26.

Please cite this article as: Nazir SM et al., Pathways to low-cost clean hydrogen production with gas switching reforming, International Journal of Hydrogen Energy, https://doi.org/10.1016/j.ijhydene.2020.01.234

[22] Zaabout A, Cloete S, Johansen ST, van Sint Annaland M, Gallucci F, Amini S. Experimental demonstration of a novel gas switching combustion reactor for power production with integrated CO2 capture. Ind Eng Chem Res 2013;52(39):14241–50.
[23] Wassie SA, Gallucci F, Zaabout A, Cloete S, Amini S, van Sint Annaland M. Hydrogen production with integrated CO2 capture in a novel gas switching reforming reactor: proof-of-concept. Int J Hydrogen Energy 2017;42(21):14367–79.
[24] Nazir SM, Cloete JH, Cloete S, Amini S. Gas switching reforming (GSR) for power generation with CO2 capture: process efficiency improvement studies. Energy 2019;167:757–65.
[25] Francisco Morgado J, Cloete S, Morud J, Gurker T, Amini S. Modelling study of two chemical looping reforming reactor configurations: looping vs. switching. Powder Technol 2017;316:599–613.
[26] Nazir SM, Cloete S, Bolland O, Amini S. Techno-economic assessment of the novel gas switching reforming (GSR) concept for gas-fired power production with integrated CO2 capture. Int J Hydrogen Energy 2018;43(18):8754–69.
[27] Szima S, Nazir SM, Cloete S, Amini S, Fogarasi S, Cormos A-M, et al. Gas switching reforming for flexible power and hydrogen production to balance variable renewables. Renew Sustain Energy Rev 2019;110:207–19.
[28] IEAGHG. CCS in energy and climate scenarios. 2019.
[29] Nazir SM, Cloete JH, Cloete S, Amini S. Efficient hydrogen production with CO_2 capture using gas switching reforming (GSR): techno-economic assessment. In: Stanek W, Gładysz P, Werle S, Adamczyk W, editors. The 32nd international conference on efficiency, cost, optimization, simulation and environmental impact of energy systems (ECOS). Wroclaw, Poland; 2019. p. 635–44.
[30] Cloete S, Romano MC, Chiesa P, Lozza G, Amini S. Integration of a Gas Switching Combustion (GSC) system in integrated gasification combined cycles. Int J Greenhouse Gas Control 2015;42:340–56.
[31] AspenHYSYS. Aspen, HYSYS V8.6 user guide. Bedford, Massachusetts, USA: Aspen Technology Inc.; 2017.
[32] EBTF. European best practice guidelines for assessment of CO2 capture technologies. CESAR -project 7th FrameWork Programme. Collaborative Project– GA No. 213569; 2011.
[33] GCCSI. Global CCS Institute - toward a common method OF cost estimation for CO2 capture and storage at fossil fuel power plants. 2013.
[34] RSMeans. 2019. https://www.rsmeansonline.com/references/unit/refpdf/hci.pdf. [Accessed 17 September 2019].
[35] Thermoflow. Thermoflow, Suite V26 user guide. Southborough, MA, USA: Thermoflow Inc.; 2017.
[36] Turton R, Bailie R, Whiting W, Shaeiwitz J. Analysis, synthesis and design of chemical processes. Pearson Education; 2008.
[37] Ugwu A, et al. Gas Switching Reforming for syngas production with iron-based oxygen carrier-the performance under pressurized conditions. Int J Hydrogen Energy 2020;45(2):1267–82.
[38] DOE/NETL. Cost estimation methodology for NETL assessments of power plant performance. 2011.
[39] Alibaba. Pingxiang Gophin Chemical Co., Ltd; 2020. Supplier, https://www.alibaba.com/product-detail/Drying-Agent-PSA-Oxygen-Concentrator-5A_60735393701.html?spm=a2700.7724838.0.0.5c351944VxSflb. [Accessed 7 January 2020].
[40] Alibaba. Ningxia Yongruida Carbon Co., Ltd; 2020. Supplier, https://www.alibaba.com/product-detail/Water-Gas-Treatment-adsorbent-Activated-Charcoal_62143077960.html?spm=a2700.7724838.0.0.4f762ddatFq25V. [Accessed 7 January 2020].
[41] Cloete S, Khan MN, Amini S. Economic assessment of membrane-assisted autothermal reforming for cost effective hydrogen production with CO2 capture. Int J Hydrogen Energy 2019;44(7):3492–510.
[42] Roussanaly S, Bureau-Cauchois G, Husebye J. Costs benchmark of CO2 transport technologies for a group of various size industries. Int J Greenhouse Gas Control 2013;12:341–50.
[43] https://www.statista.com/statistics/252791/natural-gas-prices/. [Accessed 22 November 2019].
[44] Johansson D, Sjöblom J, Berntsson T. Heat supply alternatives for CO2 capture in the process industry. Int J Greenhouse Gas Control 2012;8:217–32.
[45] IRENA. Renewable power generation costs in 2017. Abu Dhabi: International Renewable Energy Agency; 2018.
[46] Cloete S, Hirth L. Flexible power and hydrogen production: finding synergy between CCS and variable renewables. Energy 2020;192:116671.

Please cite this article as: Nazir SM et al., Pathways to low-cost clean hydrogen production with gas switching reforming, International Journal of Hydrogen Energy, https://doi.org/10.1016/j.ijhydene.2020.01.234